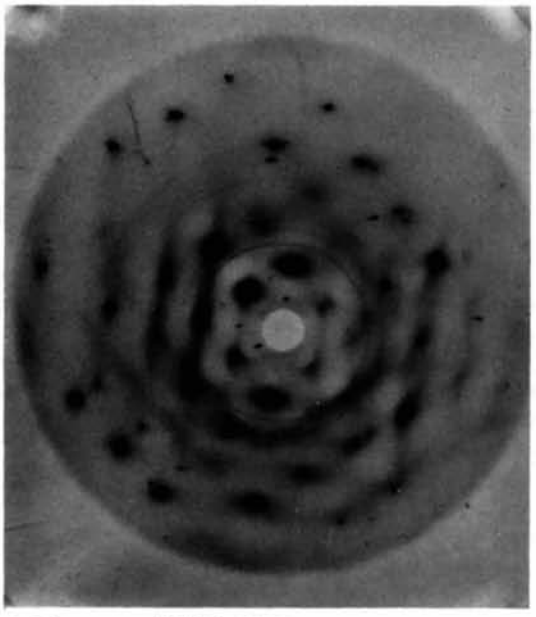

Fig. 4. Diagramme réalisé à 433 K avec un rayonnement Mo $K\alpha$. L'axe [00.1] est perpendiculaire au faisceau incident.

Un autre point nous frappe dans la comparaison des deux phases, pour laquelle nous avons donné un tableau récapitulatif (Fig. 3):

– l'orientation plus symétrique des NO_3 dans la phase haute température entraîne une plus grande homogénéité des liaisons. Comme nous l'avons vu, chaque atome d'argent est lié à neuf oxygènes [Fig. 3(1*d*)] alors que pour la phase métastable il n'est lié qu'à six oxygènes avec une répartition des liaisons plus anisotropes [Fig. 3(2*d*)]. Inversement, chaque oxygène est lié à trois atomes d'argent dans la phase haute température [Fig. 3(1*c*)] et seulement à deux dans la phase métastable [Fig. 3(2*c*)]. On peut donc concevoir que l'empilement de la phase haute température est 'mécaniquement' plus stable que celui de la phase métastable.

L'examen de cette structure nous a fait entrevoir la possibilité d'un désordre (orientation des NO_3 par rapport à celle de la phase métastable, décalage des groupements NO_3 par rapport au centre du rhomboèdre pouvant entraîner une juxtaposition de mailles 'droites' et de mailles 'gauches', soit dans un désordre total, soit sous forme de domaines).

Nous avons effectivement pu mettre en évidence des traînées de diffusion visibles sur un diagramme de 'Laue monochromatique', réalisé par Françoise Denoyer (Fig. 4).

L'interprétation de cette diffusion demande une étude plus approfondie.

Références

BUSING, W. R., MARTIN, K. O. & LEVY, H. A. (1962). *ORFLS*. Report ORNL-TM-305. Oak Ridge National Laboratory, Tennessee.

MEYER, P., RIMSKY, A. & CHEVALIER, R. (1976). *Acta Cryst.* B**32**, 1143–1146.

MEYER, P., RIMSKY, A. & CHEVALIER, R. (1978). *Acta Cryst.* B**34**, 1457–1462.

PISTORIUS, C. W. E. T. (1961). *Z. Kristallogr.* **115**, 291–296.

Acta Cryst. (1982). B**38**, 2546–2554

The Structure of $UO_2DAsO_4.4D_2O$ at 4 K by Powder Neutron Diffraction

BY A. N. FITCH, A. F. WRIGHT AND B. E. F. FENDER

Institut Laue–Langevin, 156X Centre de Tri, 38042 *Grenoble, France*

(*Received* 6 *February* 1982; *accepted* 28 *April* 1982)

Abstract

The low-temperature structure of deuterated uranyl hydrogenarsenate tetrahydrate, $UO_2DAsO_4.4D_2O$, has been determined in space group $P\bar{1}$ with a = 7·1644 (1), b = 7·1124 (1), c = 17·5537 (3) Å, α = 90·187 (3), β = 89·947 (4), γ = 90·003 (4)° and $Z = 4$ from profile analysis of a powder neutron diffraction pattern at 4 K. The profile arising from 2098 overlapping reflections, including 41 reflections from contaminating ice, was refined to an R_{wp} of 4·19 using a new computer program which allows the simultaneous refinement of more than one phase. The structure consists of chains of H_4O_2 dimers and $H_5O_2^+$ ions which alternate between layers of UO_2^{2+} and AsO_4^{3-} ions.

0567-7408/82/102546-09$01.00

Introduction

At room temperature the isostructural layered compounds $UO_2HAsO_4.4H_2O$ (HUAs) and $UO_2HPO_4.4H_2O$ (HUP) show very high proton conductivity parallel to the basal plane as a bulk property of the crystals (Shilton & Howe, 1977; Howe & Shilton, 1979, 1980). Childs, Halstead, Howe & Shilton (1978) confirm by pulsed proton NMR that hydrogen diffusion in these compounds is very rapid with an activation energy of 20 ± 1 kJ mol^{-1}. Single-crystal X-ray studies by Morosin (1978*a*,*b*) on HUP at room temperature located the positions of all the atoms except hydrogen in space group *P*4/*ncc*. The structure consists of two-dimensional networks of water molecules grouped into squares (plus the remaining H^+ ion), which alternate between layers of UO_2^{2+} and PO_4^{3-} ions. A network of hydrogen bonds connects the water molecules to each other and to the oxygen atoms of the phosphate groups. Every water molecule may participate in four hydrogen bonds, so for every four water oxygens in a square there are only nine hydrogen atoms to be distributed over the ten possible sites.

Bernard, Fitch, Howe, Wright & Fender (1981), from powder neutron diffraction studies on $UO_2DAsO_4.4D_2O$ at room temperature, confirmed that DUAs was isostructural with HUP and determined how the various hydrogen-bond sites were occupied, Fig. 1. The hydrogen-bond site joining water molecules within a square is found to be $\frac{3}{4}$ occupied with 12 hydrogens distributed statistically over the 16 possible sites per unit cell. The average unit cell can then be described in terms of the presence of two types of water species, $H_5O_2^+$ and H_4O_2 dimers, which are disordered at this temperature. The dynamic interchange between these two units provides a simple mechanism for hydrogen-ion mobility in this compound.

Both the conductivity and NMR measurements show that HUP and HUAs undergo a transition, the former at 274 K and the latter at 301 K, to a poorly-conducting low-temperature phase. For HUAs this coincides with the paraelectric-to-antiferroelectric transition observed by de Benyacar & de Dussel (1975).

Using X-ray powder diffraction, differential scanning calorimetry (DSC) and infrared spectroscopy, Shilton & Howe (1980) have investigated the nature of these transitions. At 305 K the X-ray powder pattern of HUAs was compatible with space group *P*4/*ncc* with $a = 7{\cdot}150\ (2)$ and $c = 17{\cdot}608\ (5)$ Å. On cooling to 293 K a change to 'orthorhombic' symmetry was observed with $a = 7{\cdot}128\ (2)$, $b = 7{\cdot}168\ (2)$ and $c = 17{\cdot}613\ (5)$ Å. At 260 K HUP is also 'orthorhombic' with $a = 6{\cdot}966\ (5)$, $b = 7{\cdot}004\ (5)$ and $c = 17{\cdot}43\ (1)$ Å.

Below their transition temperatures the crystals appear as two sets of anisotropic domains oriented at approximately 90° to each other with domain walls parallel to (110) of the original tetragonal cell, and subdomain boundaries parallel to (010). de Benyacar & de Dussel (1978), from detailed observations of the domain and subdomain structure of HUAs below the transition temperature, suggest that the antiferroelectric phase must crystallize in point groups 1, $\bar{1}$, 2 or 222. Shilton & Howe (1979), as a result of their observed 'orthorhombic' unit cell, have proposed an ordered hydrogen-bonded structure based on the original-sized unit cell consistent with 222 in space group $P2_12_12$, which is a subgroup of *P*4/*ncc*. In a paraelectric-to-antiferroelectric transition a multiple

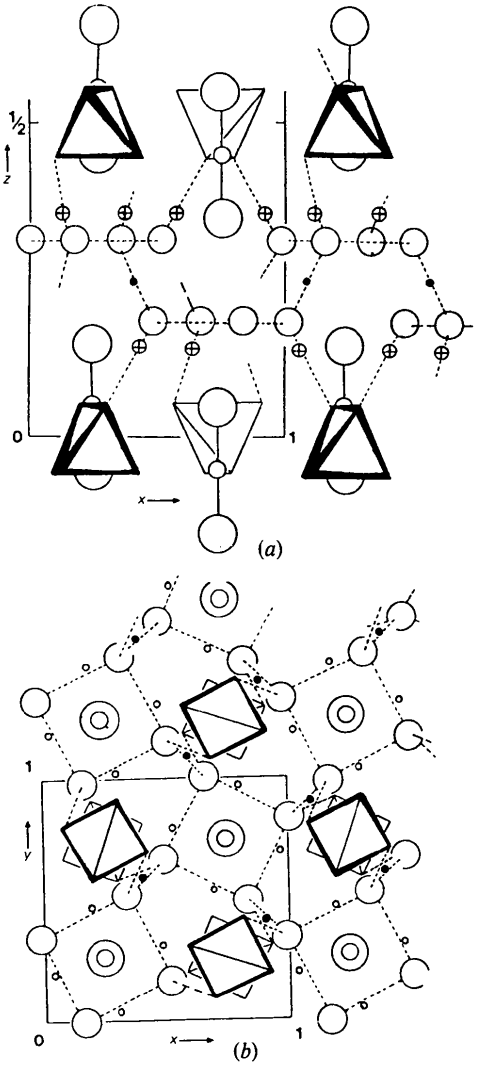

Fig. 1. Projection of the structure of $UO_2DAsO_4.4D_2O$ at 305 K along (*a*) [010], H(1) hydrogens not shown; and (*b*) [001], H(2) hydrogens not shown. Large open circles: uranyl oxygens; medium open circles: water oxygens; tetrahedra: arsenate groups; smaller open circles: uranium; small black circles: H(3) hydrogens; smallest open circles: H(1) hydrogens; crossed circles: H(2) hydrogens (Fitch *et al.*, 1982).

unit cell usually results (Zheludev, 1971), although if the original paraelectric cell contains an even number of equivalent 'molecules' this may not be necessary in order to realize the superstructure characteristic of an antiferroelectric phase (Känzig, 1957).

DSC gives an upper limit to the enthalpy of transition of 0·5 kJ mol^{-1} of water. IR spectroscopy gave evidence for the presence of H_3O^+ ions in both compounds above and below the transitions, although the occurrence of peaks in the region 2200–2300 cm^{-1} is compatible with the presence of $H_5O_2^+$ ions.

In the absence of an electric field applied parallel with the c axis of the room-temperature phase, powder X-ray diffraction, DSC (Shilton & Howe, 1980) and our own neutron diffraction studies give no evidence for the ferroelectric transition to a structure in point group 1 reported by de Benyacar & de Dussel (1975, 1978) at 253 K.

Experimental

A sample, 8·61 g of deuterated $UO_2DAsO_4.4D_2O$, was prepared by Dr M. G. Shilton by standard techniques and sealed in a thin-walled vanadium can. Neutron powder diffraction studies at a wavelength of 1·9094 Å were performed at 4 K on the high-resolution powder diffractometer D1A at the High Flux Reactor at ILL (Grenoble). The sample was contained in the standard liquid-helium cryostat. Diffraction data were collected in steps of 0·05° over an angular range between 1 and 160° in 2θ. The scan took about 24 h.

Structural refinement

The diffraction pattern of DUAs at 4 K is more complex than at room temperature (Fitch, Bernard, Howe, Wright & Fender, 1982), with obvious splitting of certain peaks, as was reported earlier by Shilton & Howe (1980). The latter's postulated model in the orthorhombic space group $P2_12_12$, however, cannot be correct due to the presence of a weak peak at 15·3° which may be indexed as 010. There were no visible supercell reflections.

To ensure that the structure determination was of the fully hydrated compound, the sample had been sealed in its vanadium can whilst still slightly wet. As a result, a number of peaks from deuterated ice were visible in the pattern. In fact altogether there were 41 ice peaks within the observed 2θ range and we have, therefore, used the profile analysis program (Rietveld, 1967, 1969) which has been modified by Thomas & Bendall (1978) to allow simultaneous refinement of more than one phase contributing to a single profile (Bendall, 1980). This program has been previously used for the refinement of Na_2UCl_6 with NaCl and Li_2UCl_6 with LiCl (Bendall, Fitch & Fender, 1982).

The Rietveld method minimizes the function

$$\chi^2 = \sum_i w_i |y_i(\text{obs}) - (1/c)\, y_i(\text{calc})|^2,$$

where $y_i(\text{obs})$, $y_i(\text{calc})$, and c are the observed intensity at the position 2θ, the calculated intensity and the single scale factor for the profile respectively. The assigned weight is $w_i = n/(y_i + B_i)$, where y_i is the value of the profile point before subtraction of the estimated background B_i and n is the number of counters contributing to y_i (Hewat & Bailey, 1976). The program calculates three R factors:

the profile R factor,

$$R_p = 100 \sum_i |y_i(\text{obs}) - (1/c)y_i(\text{calc})| \Big/ \sum_i y_i(\text{obs});$$

the weighted profile R factor,

$$R_{wp} = 100 \left\{ \sum_i w_i [y_i(\text{obs}) - (1/c)y_i(\text{calc})]^2 \Big/ \sum_i w_i [y_i(\text{obs})]^2 \right\}^{1/2};$$

and an R factor based on estimates of the observed integrated intensities, obtained by partitioning the pattern according to the values calculated,

$$R_I = 100 \sum_k |I_k(\text{obs}) - (1/c)I_k(\text{calc})| \Big/ \sum_k I_k(\text{obs}).$$

There is also an expected R factor:

$$R_E = 100 \left\{ (N - P + C) \Big/ \sum_i w_i [y_i(\text{obs})]^2 \right\}^{1/2},$$

which we might expect to obtain were differences between the observed and calculated profiles only statistical in origin. The quantity $N - P + C$ is the number of degrees of freedom where N is the number of statistically independent observations, P is the number of least-squares parameters and C the number of constraint functions. The scattering lengths used were U 8·50, As 6·40, O 5·80, D 6·67 fm (Bacon, 1975).

In all the refinements for DUAs, the 41 ice peaks were accounted for by refining a contribution due to this phase in space group $P6_3/mmc$ (Peterson & Levy, 1957). This requires an effective relative scale factor, two lattice parameters, three half-width parameters, a single isotropic temperature factor for both crystallographically distinct hydrogen atoms, an isotropic temperature factor for oxygen and atomic positional parameters which are given by Peterson & Levy (1957) at 123 K as:

D(1)	4(*f*)	$\frac{1}{3}$	$\frac{2}{3}$	z		$z = 0{\cdot}1980\ (7)$; occupancy = 2
D(2)	12(*k*)	x	$2x$	z	$x = 0{\cdot}4545\ (9)$;	$z = 0{\cdot}0172\ (4)$; occupancy = 6
O	4(*f*)	$\frac{1}{3}$	$\frac{2}{3}$	z		$z = 0{\cdot}0620\ (4)$; occupancy = 4,

i.e. a total of 12 parameters exclusive to ice. In addition, in each refinement there was a single scale factor, zeropoint and asymmetry parameter for the *pattern*. For DUAs there was the appropriate number of atomic positional and thermal parameters, the lattice parameters, three half-width parameters, a preferred orientation parameter applied with normal [001], and finally the scattering length of deuterium.

Since there are no visible superlattice peaks, only models based on the original-sized unit cell were examined. Space groups compatible with the point-group proposals of de Benyacar & de Dussel (1978) are possible, but there is no suitable orthorhombic or higher-symmetry space group which fits a sensible structure and the observed reflections. The structure must then be monoclinic or triclinic, which requires a model with more reflections and more parameters than the standard multipattern profile refinement program (Thomas & Bendall, 1978) can handle. The program was, therefore, redimensioned to accommodate up to 3000 reflections, 300 independent parameters, 100 crystallographically distinct atoms, with a maximum of 60 reflections contributing to any single data point.

Because we need to account for the displacive transition from the room-temperature structure with ordering of the hydrogen-bond network, only space groups which were subgroups of $P4/ncc$ were considered. A first refinement was attempted in $P2_1/c$ which provides the simplest structural model conforming to our criteria (although it is incompatible with the arguments of de Benyacar & de Dussel, 1978). The hydrogen atoms H(1) within the squares of water molecules were arbitrarily ordered over three of the four possible hydrogen-bond sites so as to simulate ordering $H_5O_2^+$ and H_4O_2 units at opposite corners of the water squares. All atoms were placed in general positions 4(*e*) (*xyz*), with isotropic temperature factors which were constrained to be equal for all atoms which were symmetrically equivalent at room temperature. With 72 atomic parameters for DUAs (making a total of 96 variables and 1073 reflections), the refinement terminated with $R_{wp} = 16{\cdot}13$ and $R_E = 3{\cdot}04$. There were negative temperature factors for U, As, O(1) and O(3). The values of the positional parameters were not unreasonable, but the high R_{wp} and negative temperature factors indicate an unsatisfactory refinement.

Reducing the symmetry to $P2_1$ or Pc (the latter again disallowed by de Benyacar & de Dussel, 1978) doubles the number of crystallographically distinct atoms. A similar regime of atomic positions and temperature factors was followed as for $P2_1/c$, to give in each case 135 atomic parameters for DUAs and a total of 159 variables. The program consistently failed with a singular least-squares matrix, which may have been due to strong correlations between parameters as a result of an improperly chosen space group, or possibly because the sheer size of the normal matrix makes it very

Table 1. *Final parameters for* $UO_2DAsO_4.4D_2O$ *at* 4 K *in space group* $P\bar{1}$

E.s.d.'s of refined parameters are in parentheses. The atoms are labelled so that they may easily be compared with the room-temperature structure (Morosin, 1978*a*; Fitch *et al.*, 1982). Thus O(4) = water oxygen; O(3) = arsenate oxygen; O(1) and O(2) = uranyl oxygens; H(1) = in-square hydrogen; H(2) = arsenate hydrogen; H(3) = hydrogen linking adjacent water squares. The system of subscripts is devised so that atoms which are most closely bonded to a particular water oxygen all have the same subscript. Hence water oxygen $O(4)_{A2}$ is directly attached to hydrogens $H(1)_{A2}$ and $H(2)_{A2}$ and hydrogen bonded [*via* $H(2)_{A2}$] to arsenate oxygen $O(3)_{A2}$. $O(3)_{A2}$ is itself bonded to As(2) and coordinates U(2) to which are attached $O(1)_2$ and $O(2)_2$.

	x	y	z	B_{iso} (Å^2)
U(1)	0·742 (1)	0·750 (2)	0·4466 (6)	0·07 (4)
U(2)	0·256 (1)	0·250 (2)	0·0549 (6)	0·07 (4)
As(1)	0·752 (2)	0·250 (2)	0·5004 (9)	0·21 (6)
As(2)	0·756 (2)	0·255 (2)	0·0029 (9)	0·21 (6)
$O(1)_1$	0·746 (2)	0·751 (2)	0·3451 (11)	0·35 (7)
$O(1)_2$	0·251 (2)	0·249 (2)	0·1562 (11)	0·35 (7)
$O(2)_1$	0·259 (2)	0·252 (3)	0·4510 (9)	0·13 (7)
$O(2)_2$	0·757 (2)	0·743 (3)	0·0463 (9)	0·13 (7)
$O(3)_A$	0·072 (2)	0·795 (2)	0·4399 (9)	0·17 (4)
$O(3)_{A2}$	0·557 (2)	0·196 (2)	0·0543 (9)	0·17 (4)
$O(3)_B$	0·426 (2)	0·691 (2)	0·4387 (9)	0·17 (4)
$O(3)_{B2}$	0·930 (2)	0·300 (2)	0·0604 (9)	0·17 (4)
$O(3)_C$	0·791 (2)	0·424 (2)	0·4391 (7)	0·17 (4)
$O(3)_{C2}$	0·298 (2)	0·564 (2)	0·0515 (7)	0·17 (4)
$O(3)_D$	0·694 (2)	0·063 (2)	0·4429 (9)	0·17 (4)
$O(3)_{D2}$	0·191 (2)	0·930 (2)	0·0528 (9)	0·17 (4)
$O(4)_A$	0·142 (2)	0·994 (3)	0·3116 (10)	0·72 (4)
$O(4)_{A2}$	0·629 (2)	0·995 (3)	0·1881 (10)	0·72 (4)
$O(4)_B$	0·354 (2)	0·496 (3)	0·3096 (10)	0·72 (4)
$O(4)_{B2}$	0·843 (2)	0·492 (3)	0·1894 (9)	0·72 (4)
$O(4)_C$	0·893 (1)	0·296 (2)	0·2970 (8)	0·72 (4)
$O(4)_{C2}$	0·423 (2)	0·697 (2)	0·1989 (9)	0·72 (4)
$O(4)_D$	0·484 (2)	0·166 (3)	0·3106 (10)	0·72 (4)
$O(4)_{D2}$	0·994 (2)	0·834 (3)	0·1872 (10)	0·72 (4)
$H(1)_A$	0·272 (2)	0·051 (3)	0·3116 (12)	1·45 (5)
$H(1)_{A2}$	0·761 (2)	0·955 (3)	0·1874 (12)	1·45 (5)
$H(1)_B$	0·415 (2)	0·373 (3)	0·3118 (11)	1·45 (5)
$H(1)_{B2}$	0·906 (2)	0·623 (3)	0·1901 (11)	1·45 (5)
$H(1)_C$	0·996 (2)	0·202 (2)	0·3044 (10)	1·45 (5)
$H(1)_{C2}$	0·505 (2)	0·807 (2)	0·1951 (10)	1·45 (5)
$H(2)_A$	0·122 (2)	0·922 (2)	0·3558 (10)	1·32 (5)
$H(2)_{A2}$	0·617 (2)	0·051 (2)	0·1399 (10)	1·32 (5)
$H(2)_B$	0·380 (2)	0·565 (2)	0·3576 (11)	1·32 (5)
$H(2)_{B2}$	0·879 (2)	0·428 (2)	0·1395 (12)	1·32 (5)
$H(2)_C$	0·885 (2)	0·342 (2)	0·3517 (9)	1·32 (5)
$H(2)_{C2}$	0·379 (2)	0·643 (2)	0·1504 (9)	1·32 (5)
$H(2)_D$	0·565 (2)	0·135 (2)	0·3568 (11)	1·32 (5)
$H(2)_{D2}$	0·060 (2)	0·855 (2)	0·1395 (11)	1·32 (5)
$H(3)_B$	0·389 (2)	0·578 (2)	0·2650 (8)	1·40 (8)
$H(3)_{B2}$	0·881 (2)	0·395 (2)	0·2418 (9)	1·40 (8)
$H(3)_D$	0·565 (3)	0·111 (2)	0·2665 (10)	1·40 (8)
$H(3)_{D2}$	0·056 (3)	0·876 (2)	0·2294 (10)	1·40 (8)

difficult to invert (Acton, 1970). A progressive reduction of the R factor could be obtained, however, if the refinements were carried out in two stages, the first involving 85 variables and fixed uranyl and arsenate atomic parameters, followed by a second step with 87 variables and the atomic parameters of water fixed. For $P2_1$, with 1178 total reflections, the best fit produced $R_{wp} = 12{\cdot}81$, $R_E = 3{\cdot}05$, but with negative temperature factors on As and O(2). The refinement in Pc with 1077 reflections resulted in $R_{wp} = 12{\cdot}85$, $R_E = 3{\cdot}03$ but with negative temperature factors on several atoms. Neither of these models was considered satisfactory.

The inclusion of two extra lattice parameters provided in space group $P\bar{1}$ led to a dramatic improvement in the fit. With a total of 2098 reflections, the 161 variables could all be refined simultaneously and terminated with $R_{wp} = 4{\cdot}14$, $R_E = 3{\cdot}00$, $R_p = 4{\cdot}37$, $R_I = 2{\cdot}57$. It should be noted that the unit-cell axes for the structure in $P\bar{1}$ are chosen so as to be easily compared to those of the room-temperature tetragonal phase. For the monoclinic models discussed earlier, if the monoclinic space group is used in the more usual second setting, with the b axis unique, interchange of the x and y directions for $P\bar{1}$ is necessary. Alternatively, the monoclinic unit cell may be referred to a set of axes comparable to those for $P\bar{1}$, but in this case the a axis must be taken as unique.

The observed, calculated and difference profiles are shown in Fig. 2;* the final parameters in Table 1. All the temperature factors are sensible and the occupancy of deuterium indicated that deuteration was 98 ± 1%. A Fourier map based on 'observed' intensities and calculated phases was in very good agreement with the final atomic parameters, and a difference map showed no peaks of intensity greater than 1·3% of the maximum observed peak. A Fourier difference map, however, is not wholly definitive, for in profile refinement the partitioning of the scattered intensity between overlapping peaks is done on the basis of the calculated model. In the present case, where there is extreme overlap of reflections with an average of about 2·4 profile points per reflection up to 80° in 2θ, and 1·0 profile points per reflection thereafter, strong biasing to the calculated model is possible.

With such a large number of parameters, could *any* profile pattern be fitted to a reasonable degree of accuracy? We argue, however, that the models in $P2_1$ and Pc each have only two fewer parameters than $P\bar{1}$ and yet give a much worse fit. In fact all three models describe the same qualitative arrangement of atoms and they differ essentially in the symmetry relationship between the various groups of atoms. The large difference in R factor between the triclinic and monoclinic models is clear evidence that the former is a far superior description, and the parameters themselves are of structural significance.

* The numbered intensity of each measured point on the profile, as a function of θ, has been deposited with the British Library Lending Division as Supplementary Publication No. SUP 36930 (7 pp.). Copies may be obtained through The Executive Secretary, International Union of Crystallography, 5 Abbey Square, Chester CH1 2HU, England.

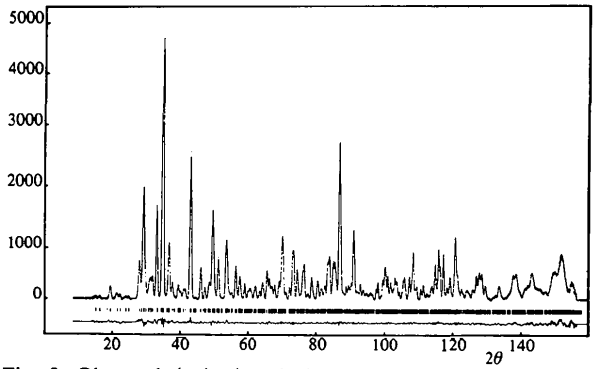

Fig. 2. Observed (points), calculated (full curve) and difference profiles for $UO_2DAsO_4.4D_2O$ at 4 K on D1A at 1·9094 Å.

Errors

Sakata & Cooper (1979) have drawn attention to the difficulty in assessing the accuracy of structural parameters obtained by profile refinement. They considered that correlations between profile points in a single Bragg peak, which were treated as independent observations, gave rise to statistical errors which may become more important with peak overlap. The credibility of the DUAs refinement can, however, be gauged by the simultaneous refinement of the known ice structure. The structural information concerning ice is incorporated with a high density of profile points from DUAs. If this information can be satisfactorily extracted by the profile refinement, we might expect that the structural information for DUAs itself could likewise be obtained. Large errors in the DUAs structure would lead to a poor fit to the observed profile. In this case compensation from the contribution to the calculated profiles from the ice would be reflected in significant deviations from the known ice structural and thermal parameters.

The final parameters, bond lengths and bond angles for ice, compared with some other values found in the literature, are given in Tables 2 and 3. The agreement is quite good although we observe that there are differences of several standard deviations with the best single-crystal data. It has to be remembered, however, that the atomic parameters for ice are determined wholly from weak peaks in the diffraction pattern, which contribute only 5·4% of the total Bragg intensity. Also, our model involves only isotropic temperature factors. Nevertheless we recognize from the ice refinements that the quoted errors may also be underestimated in the major-phase DUAs. Even so, if we use ice as a guide,

the O–D and O---O distances in DUAs are unlikely to be in error by more than about 0·05 Å with bond angles good to at least 2°. The lattice parameters of ice, $a = 4{\cdot}5050\ (7)$, $c = 7{\cdot}3347\ (5)$ Å, are well determined with $c/a = 1{\cdot}6281\ (4)$ which compares well with the result of Brill & Tippe (1967) who at 13 K give $c/a = 1{\cdot}6278$ for H_2O.

Discussion

Some actual and average bond angles and distances for DUAs at 4 K are compared in Tables 4 and 5 with the values obtained at room temperature by Fitch *et al.* (1982). Although the uranyl arsenate framework is somewhat distorted from that at room temperature in this low-temperature phase, the arrangement of atoms is very similar and the average interatomic distances and angles are only slightly altered. For the water layers there are more significant changes with ordering of the three H(1) hydrogens over the four possible sites per water square. Fig. 3 shows the new arrangement of

Table 2. *Final atomic parameters for deuterated ice at 4 K compared with some others taken from the literature*

E.s.d.'s are in parentheses. B values are in Å^2.

	4 K[a]	123 K[b]	223 K[b]
z D(1)	0·205 (1)	0·1980 (7)	0·1989 (9)
x D(2)	0·454 (1)	0·4545 (9)	0·4551 (13)
z D(2)	0·017 (1)	0·0172 (4)	0·0182 (6)
z O	0·066 (1)	0·0620 (4)	0·0629 (6)
B D	2·2 (2)	—	—
B O	1·2 (1)	—	—
B_{11} D(1)	—	2·41 (13)	3·23 (22)
B_{33} D(1)	—	1·81 (12)	2·97 (28)
B_{11} D(2)	—	2·29 (21)	3·30 (27)
B_{22} D(2)	—	1·85 (12)	2·80 (26)
B_{33} D(2)	—	2·43 (10)	3·05 (15)
B_{13} D(2)	—	0·24 (18)	0·24 (18)
B_{11} O	—	1·53 (11)	2·39 (22)
B_{33} O	—	1·48 (10)	2·29 (17)

References: (*a*) this work; (*b*) Peterson & Levy (1957), single crystal, D_2O.

Table 4. *Bond distances* (Å) *and angles* (°) *for the uranyl arsenate framework in* $UO_2DAsO_4.4D_2O$ *at* 4 K, *compared with the values at room temperature*

E.s.d.'s are in parentheses. For certain bond types, only the extreme and average values are given. In these cases, 'X' stands for either A, B, C or D.

	Value(s)	Average	Room temperature
Uranyl ion			
$U(1)–O(1)_1$	1·78 (2)	1·78 (2)	1·796 (3)
$U(2)–O(1)_2$	1·78 (2)		
$U(1)–O(2)_1$	1·80 (2)		
$U(2)–O(2)_2$	1·78 (2)	1·79 (2)	1·781 (4)
$O(1)_1–U(1)–O(2)_1$	179·5 (10)	177·5 (10)	180
$O(1)_2–U(2)–O(2)_2$	175·6 (10)		
$U(1)–O(3)_A$	2·39 (2)		
$U(1)–O(3)_B$	2·31 (2)	2·33 (2)	2·303 (1)
$U(1)–O(3)_C$	2·35 (2)		
$U(1)–O(3)_D$	2·26 (2)		
$U(2)–O(3)_{A2}$	2·19 (2)		
$U(2)–O(3)_{B2}$	2·36 (2)	2·28 (2)	2·303 (1)
$U(2)–O(3)_{C2}$	2·26 (2)		
$U(2)–O(3)_{D2}$	2·32 (2)		
$O(1)_1–U(1)–O(3)_X$	86·3 (7)–88·1 (7)	87·2 (7)	88·0 (6)
$O(2)_1–U(1)–O(3)_X$	92·3 (8)–93·7 (7)	92·8 (8)	92·00 (6)
$O(1)_2–U(2)–O(3)_{X2}$	86·6 (7)–92·0 (8)	90·1 (8)	88·0 (6)
$O(2)_2–U(2)–O(3)_{X2}$	87·0 (8)–93·0 (8)	89·9 (8)	92·00 (6)
Arsenate ion			
$As(1)–O(3)_X$	See Table 5	1·70 (2)	1·680 (1)
$As(2)–O(3)_{X2}$	See Table 5	1·68 (2)	1·680 (1)
$O(3)_A–As(1)–O(3)_B$	102·5 (11)	103·1 (11)	106·00 (7)
$O(3)_C–As(1)–O(3)_D$	103·6 (11)		
$O(3)_A–As(1)–O(3)_C$	115·1 (10)		
$O(3)_A–As(1)–O(3)_D$	113·8 (11)	112·7 (10)	111·23 (6)
$O(3)_B–As(1)–O(3)_C$	110·2 (10)		
$O(3)_B–As(1)–O(3)_D$	111·8 (10)		
$O(3)_{A2}–As(2)–O(3)_{B2}$	110·6 (12)	109·8 (12)	106·00 (7)
$O(3)_{C2}–As(2)–O(3)_{D2}$	109·0 (11)		
$O(3)_{A2}–As(2)–O(3)_{C2}$	107·4 (9)		
$O(3)_{A2}–As(2)–O(3)_{D2}$	107·5 (10)	109·3 (10)	111·23 (6)
$O(3)_{B2}–As(2)–O(3)_{C2}$	112·4 (11)		
$O(3)_{B2}–As(2)–O(3)_{D2}$	109·8 (10)		
$U(1)–O(3)_X–As(1)$	130·4 (10)–134·9 (10)	132·8 (10)	136·0 (1)
$U(2)–O(3)_{X2}–As(2)$	134·4 (10)–140·1 (10)	137·7 (10)	136·0 (1)

Table 3. *Bond distances* (Å) *and angles* (°) *for ice*

	4 K[a]	60 K[c]	60 K[d]	77 K[e]	123 K[b]	223 K[b]
O–O′	2·695 (7)	2·7490 (10)	2·7490	2·744 (2)	2·755 (6)	2·752 (8)
O–O″	2·777 (2)	2·7517 (6)	2·7517	2·741 (1)	2·746 (2)	2·765 (2)
O–D(1)	1·019 (10)	1·0036 (13)	1·0127	0·999 (9)	0·997 (7)	1·000 (9)
O–D(1)*	—	—	—	1·018 (9)	1·008	1·011
O–D(2)	1·009 (7)	1·0040 (6)	1·0121	1·006 (5)	0·997 (4)	1·007 (5)
O–D(2)*	—	—	—	1·023 (5)	1·009	1·015
O′–O–O″	110·49 (13)	109·34 (1)	109·35	109·33 (10)	109·30 (2)	109·55 (15)
O″–O–O‴	108·43 (12)	109·60 (2)	109·60	109·55 (18)	109·63 (2)	109·40 (2)
D(2)–O–D(2)′	108·0 (7)	109·68 (9)	110·10	109·83 (33)	109·90 (25)	109·87 (27)
D(1)–O–D(2)	110·9 (4)	109·26 (9)	108·84	109·15 (47)	109·18 (22)	109·10 (30)

References: (*a*) this work; D_2O; (*b*) Peterson & Levy (1957), single crystal, D_2O; (*c*) Kuhs & Lehmann (1981), single crystal, H_2O; (*d*) Kuhs & Lehmann (1981), with an anharmonic probability density function for hydrogen; (*e*) Chamberlain, Moore & Fletcher (1973), single crystal, D_2O.

* Corrected for thermal motion.

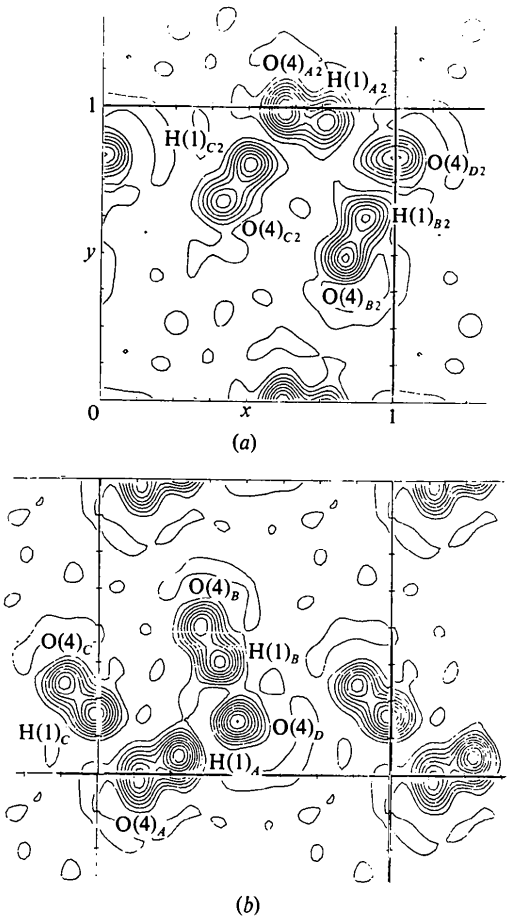

Fig. 3. Fourier sections based on observed intensities and calculated phases for $UO_2DAsO_4.4D_2O$ at 4 K, through (*a*) $z = 0{\cdot}19$ and (*b*) $z = 0{\cdot}31$, showing the arrangement of the water layers.

oxygen and hydrogen atoms at $z = 0{\cdot}19$ and $z = 0{\cdot}31$. Each 'square' possesses a hydrogen vacancy and a single water molecule whose plane runs roughly parallel to the *c* axis and has no H(1) hydrogen of its own [*i.e.* $O(4)_D$ and $O(4)_{D2}$]. The 'squares' are rather distorted and buckled compared with those at room temperature. Each water oxygen is connected to the oxygen of an arsenate group *via* a hydrogen H(2) bond and to another water molecule in the adjacent level *via* a linking H(3) hydrogen.

From Fig. 4 it can be seen that the water molecules form hydrogen-bonded chains which alternate between $z = 0{\cdot}19$ and $z = 0{\cdot}31$ *via* the H(3) linking hydrogens. Two such chains, *B* and *B'*, run in the direction of the *b* axis and are cross linked by only one chain, *A*, in the *a* direction. The intersection of two chains always involves a water molecule which has no directly bound H(1) [$O(4)_D$ or $O(4)_{D2}$] and the *A* chain may be considered as being composed of sets of two H_4O_2 dimers which are ordered such that they occupy two adjacent corners of a water 'square' (in contrast to the starting model for the structural refinement), but with reversed configurations so they are linked by a single in-square hydrogen bond. Thus water oxygens $O(4)_A$ and $O(4)_D$ each comprise part of two different adjacent H_4O_2 dimers, and are bonded in the square by hydrogen $H(1)_A$ and linked to the second oxygen of the dimer, $O(4)_{D2}$ and $O(4)_{A2}$ by $H(3)_{D2}$ and $H(3)_D$ respectively. The oxygen–oxygen distances within the dimers, 2·67 (2) and 2·68 (2) Å, are less than the distances between them, 2·86 (2) and 2·74 (2) Å, and the sequence along the *A* chain is (ignoring all hydrogens directed towards the arsenate oxygens), $--[O(4)_D{-}H(3)_D{\cdots}O(4)_{A2}{-}H(1)_{A2}]{\cdots}[O(4)_{D2}{-}H(3)_{D2}{-}-O(4)_A{-}H(1)_A]--$. There are alternating short and long hydrogen–oxygen distances along the chain as adjacent dimers occur with reversed configurations. The chain is thus essentially neutral and non-polarized.

Each of the two types of water dimer in the *A* chain also comprises part of either the *B* or *B'* chains where

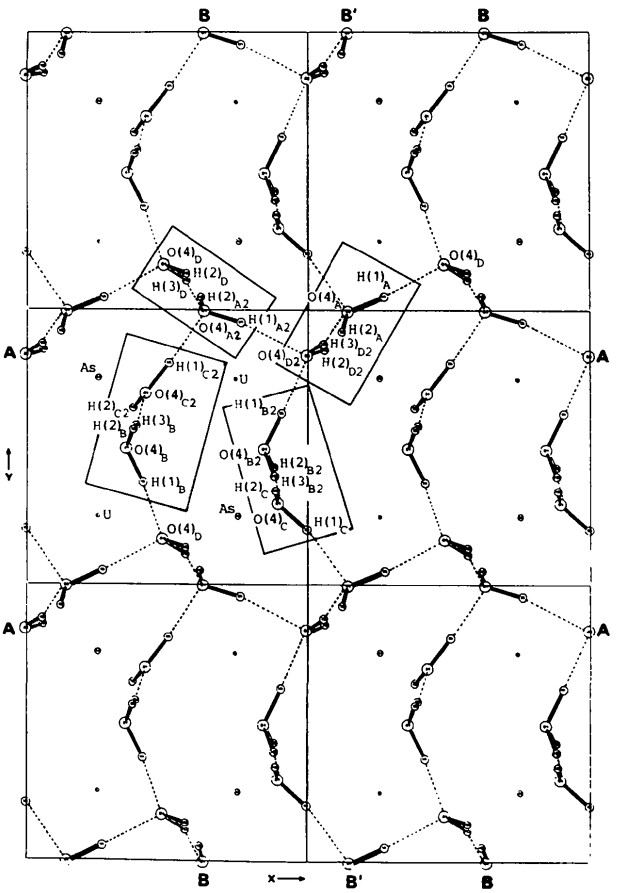

Fig. 4. Six unit cells of $UO_2DAsO_4.4D_2O$ at 4 K showing the formation of the hydrogen-bonded water chains. These run in the direction of the *b* axis from *B* to *B* and from *B'* to *B'*, and in the *a* direction from *A* to *A*.

Table 5. *Bond distances* (Å) *and angles* (°) *for the water networks in* $UO_2DAsO_4.4D_2O$ *at* 4 K

E.s.d.'s are in parentheses.

(*a*) The water molecules themselves and the hydrogen bond to the arsenate group. Mean values are compared with models *a*, *b* at 305 K

Type	O(4)–H(1)	O(4)–H(2)	O(4)–H(3)	H(2)–O(3)	O(4)–O(3)	O(3)–As	H(1)–O(4)–H(2)	H(1)–O(4)–H(3)	H(2)–O(4)–H(3)	O(4)–H(2)–O(3)
A	1·02 (2)	0·94 (2)	—	1·77 (2)	2·71 (2)	1·67 (2)	110·8 (22)	—	—	176·1 (18)
*A*2	0·99 (2)	0·92 (2)	—	1·88 (2)	2·80 (2)	1·74 (2)*	101·5 (21)	—	—	167·7 (17)
B	0·98 (3)	0·99 (3)	1·01 (2)	1·71 (2)	2·70 (2)	1·72 (2)	108·7 (22)	116·2 (21)	108·9 (22)	178·0 (20)
*B*2	1·03 (3)	1·02 (3)	1·18 (2)	1·70 (2)	2·71 (2)	1·64 (2)*	107·5 (20)	114·8 (18)	110·8 (19)	173·9 (19)
C	1·00 (2)	1·01 (2)	—	1·77 (2)	2·75 (2)	1·67 (2)	97·5 (18)	—	—	160·9 (16)
*C*2	0·98 (2)	0·98 (2)	—	1·92 (2)	2·90 (2)	1·65 (2)*	116·2 (20)	—	—	173·9 (17)
D	—	1·02 (2)	1·05 (2)	1·84 (2)	2·86 (2)	1·72 (2)	—	—	100·9 (19)	174·5 (18)
*D*2	—	0·97 (3)	0·91 (2)	1·87 (2)	2·83 (2)	1·68 (2)*	—	—	114·9 (22)	171·8 (18)
Mean	1·00 (2)	0·98 (2)	1·04 (2)	1·81 (2)	2·78 (2)	1·69 (2)	107·0 (20)	115·5 (19)	108·9 (21)	172·1 (18)
a	1·159 (7)	0·979 (4)	1·297 (4)	1·845 (3)	2·820 (4)	1·680 (1)	104·9 (4)	116·0 (3)	111·1 (3)	174·3 (3)
b	1·145 (8)	0·984 (5)	0·99 (1)	1·839 (3)	2·821 (4)	1·680 (1)	105·5 (4)	112·1 (6)	113·7 (7)	174·7 (3)

(*b*) The bonds between water oxygens to form the chains

A chain	$H(3)_D$–$O(4)_{A2}$	1·66 (2)	$O(4)_D$–$O(4)_{A2}$	2·67 (2)	$O(4)_D$–$H(3)_D$–$O(4)_{A2}$	161·5 (19)		
	$H(1)_{A2}$–$O(4)_{D2}$	1·88 (2)	$O(4)_{A2}$–$O(4)_{D2}$	2·86 (2)	$O(4)_{A2}$–$H(1)_{A2}$–$O(4)_{D2}$	169·9 (21)		
	$H(3)_{D2}$–$O(4)_A$	1·78 (2)	$O(4)_{D2}$–$O(4)_A$	2·68 (2)	$O(4)_{D2}$–$H(3)_{D2}$–$O(4)_A$	168·3 (19)		
	$H(1)_A$–$O(4)_D$	1·72 (2)	$O(4)_A$–$O(4)_D$	2·74 (2)	$O(4)_A$–$H(1)_A$–$O(4)_D$	175·2 (22)		
B chain	$O(4)_{A2}$–$H(1)_{C2}$	1·61 (2)	$O(4)_{A2}$–$O(4)_{C2}$	2·59 (2)	$O(4)_{A2}$–$H(1)_{C2}$–$O(4)_{C2}$	176·1 (17)		
	$O(4)_{C2}$–$H(3)_B$	1·46 (2)	$O(4)_{C2}$–$O(4)_B$	2·47 (2)	$O(4)_{C2}$–$H(3)_B$–$O(4)_B$	175·3 (16)		
	$H(1)_B$–$O(4)_D$	1·56 (3)	$O(4)_B$–$O(4)_D$	2·53 (3)	$O(4)_B$–$H(1)_B$–$O(4)_D$	171·1 (19)		
	$H(3)_D$–$O(4)_{A2}$	1·66 (2)	$O(4)_D$–$O(4)_{A2}$	2·67 (2)	$O(4)_D$–$H(3)_D$–$O(4)_{A2}$	161·5 (19)		
B′ chain	$O(4)_{D2}$–$H(1)_{B2}$	1·64 (3)	$O(4)_{D2}$–$O(4)_{B2}$	2·67 (2)	$O(4)_{D2}$–$H(1)_{B2}$–$O(4)_{B2}$	176·4 (19)	$H(1)_C$–$O(4)_C$–$H(2)_C$	97·5 (18)
	$H(3)_{B2}$–$O(4)_C$	1·21 (2)	$O(4)_{B2}$–$O(4)_C$	2·38 (2)	$O(4)_{B2}$–$H(3)_{B2}$–$O(4)_C$	171·1 (15)	$H(1)_C$–$O(4)_C$–$H(3)_{B2}$	123·3 (17)
	$H(1)_C$–$O(4)_A$	1·82 (2)	$O(4)_C$–$O(4)_A$	2·80 (2)	$O(4)_C$–$H(1)_C$–$O(4)_A$	166·6 (17)	$H(2)_C$–$O(4)_C$–$H(3)_{B2}$	124·5 (16)
	$O(4)_A$–$H(3)_{D2}$	1·78 (2)	$O(4)_A$–$O(4)_{D2}$	2·68 (2)	$O(4)_A$–$H(3)_{D2}$–$O(4)_{D2}$	168·3 (19)		

* O(3)–As(2) distance.

the chains intersect. The rest of the *B* and *B*′ chains is formed by an $H_5O_2^+$ ion. The extra proton is accommodated on the water molecule (*B* or *B*2) which is hydrogen bonded in the 'square' to the oxygen of a water dimer which has no H(1) hydrogen and must stabilize this configuration. The oxygen–oxygen distances within the $H_5O_2^+$ units are very short, 2·47 (2) and 2·38 (2) Å, with the effect of the extra proton being such that the distance to the water dimer of the *A* chain is generally shorter than within the dimer itself, the $O(4)_C$···$O(4)_A$ separation of 2·80 (2) Å being an exception. The sequence along the *B* chain is ··[$O(4)_D$–$H(3)_D$···$O(4)_{A2}$]···[$H(1)_{C2}$–$O(4)_{C2}$···$H(3)_B$–$O(4)_B$–$H(1)_B$]$^+$- and along *B*′, ··[$O(4)_A$···$H(3)_{D2}$–$O(4)_{D2}$]···[$H(1)_{B2}$–$O(4)_{B2}$–$H(3)_{B2}$···$O(4)_C$–$H(1)_C$]$^+$-.

For the latter chain, the linking hydrogen $H(3)_{B2}$ which joins the two water oxygens of the $H_5O_2^+$ unit [separated by 2·38 (2) Å] is situated midway or almost midway, with O–H distances of 1·18 (2) and 1·21 (2) Å and a hydrogen-bond angle of 175·3 (1·8)°. The geometry of the water molecule $O(4)_C$, unlike the neighbouring water molecule [$O(4)_{B2}$], is very distorted with H–O–H angles of 97·5 (18), 123·3(17) and 124·5 (16)°. A similar situation is observed in $HCl.2H_2O$ (Lundgren & Olovsson, 1967) which also has a very short (O···O 2·41 Å) and almost centred hydrogen bond. Here the non-symmetric $H_5O_2^+$ unit has an almost planar water molecule with H–O–H bond angles of 108, 122 and 123° and a relatively undistorted molecule with angles of 107, 109 and 111°.

In the *B* chain there is an O···O separation of 2·47 (2) Å in the $H_5O_2^+$ unit, which has the linking hydrogen $H(3)_B$ strongly displaced towards one of the water oxygens with distances of 1·01 (2) and 1·46 (2) Å, in line with the observation that one is unlikely to have a centred hydrogen bond unless the O···O separation is very close to 2·4 Å (Thomas & Liminga, 1978). Bernard *et al.* (1981) did not consider that the powder neutron diffraction data were sufficient to refine the separate atomic parameters of the H_4O_2 and $H_5O_2^+$ species, which occupy very similar regions of space at room temperature but are disordered. They were therefore unable to determine the exact nature of these species, and in particular whether the $H_5O_2^+$ unit contained a short centred and symmetric hydrogen bond. We still cannot assess whether this is the case in the room-temperature DUAs structure, although the observation that sufficiently short O···O distances may be attained, at least at low temperature, suggests more strongly the possibility.

The structure deduced for DUAs at low temperature is compatible with the other physical observations characterizing the transition. This is a displacive transition without a gross rearrangement of the atomic positions which results in a unit cell which is only very slightly distorted from the 'orthorhombic' cell observed by Shilton & Howe (1980). The ordering scheme of the hydrogen atoms leads to a large reduction in hydrogen mobility as seen from conductivity and NMR measurements, and is compatible with IR data which indicate

the presence of H_3O^+ species and that the hydrogen atoms pointing to arsenate oxygens stay firmly attached to water oxygens. de Benyacar & de Dussel (1975, 1978) observed the domain structure of the low-temperature phase, which has equal volumes of domains oriented at about 90° to one another with domain walls parallel to the tetragonal (110). The lattice parameters indicate that *a* has expanded and *b* contracted relative to the tetragonal phase. The *a* and *b* axes are crystallographically equivalent in the tetragonal system and such a distortion can occur with equal probability with the cell axes reversed, resulting in equal volumes of domains which are oriented at about 90° to one another. The (110) tetragonal planes remain almost undistorted by this model and can appear as domain walls. Each domain consists of a series of subdomains with walls parallel to the tetragonal (010). The shearing of the tetragonal cell, which is almost parallel to (010), may also occur with equal probability in either direction leaving (010) planes virtually unchanged to appear as subdomain walls.

In the high-temperature phase of DUAs, the averaging effect of the disordering of H_4O_2 and $H_5O_2^+$ results in layers of water molecules which have no net polarization. Below the transition temperature, as shown in Fig. 3 for $0 \leq z \leq 0{\cdot}5$, the extra protons are ordered and accommodated on two $H_5O_2^+$ units which occur alternately at $z \sim 0{\cdot}31$ and $z \sim 0{\cdot}19$ in the *B* and *B'* chains. These $H_5O_2^+$ units have similarities in their configuration with a resulting polarization which has a significant component along the crystallographic *a* direction. The unit cell, however, is centrosymmetric so that, for the volume $0{\cdot}5 \leq z \leq 1{\cdot}0$, there will be an equal and opposite polarization, and for the unit cell as a whole there is no net polarization. Hence our structure for DUAs at low temperature is compatible with the observed antiferroelectricity of this phase. In addition, a small, electrically induced distortion to a structure in space group *P*1 could produce the ferroelectric phase reported by de Benyacar & de Dussel (1975, 1978).

We thank Dr A. T. Howe for providing the sample and for useful discussions.

References

ACTON, F. S. (1970). *Numerical Methods that Work*, pp. 253–255. New York: Harper International.

BACON, G. E. (1975). *Neutron Diffraction*, 3rd ed., pp. 39–41. Oxford Univ. Press.

BENDALL, P. J. (1980). D.Phil. Thesis, Oxford Univ.

BENDALL, P. J., FITCH, A. N. & FENDER, B. E. F. (1982). *J. Appl. Cryst.* In the press.

BENYACAR, M. A. R. DE & DE DUSSEL, H. L. (1975). *Ferroelectrics*, **9**, 241–244.

BENYACAR, M. A. R. DE & DE DUSSEL, H. L. (1978). *Ferroelectrics*, **17**, 469–472.

BERNARD, L., FITCH, A. N., HOWE, A. T., WRIGHT, A. F. & FENDER, B. E. F. (1981). *Chem. Commun.* pp. 784–786.

BRILL, R. & TIPPE, A. (1967). *Acta Cryst.* **23**, 343–345.

CHAMBERLAIN, J. S., MOORE, F. H. & FLETCHER, N. H. (1973). *Physics and Chemistry of Ice*, edited by E. WHALLEY, S. J. JONES & L. W. GOLD, pp. 283–284. Ottawa: Royal Society of Canada.

CHILDS, P. E., HALSTEAD, T. K., HOWE, A. T. & SHILTON, M. G. (1978). *Mater. Res. Bull.* **13**, 609–619.

FITCH, A. N., BERNARD, L., HOWE, A. T., WRIGHT, A. F. & FENDER, B. E. F. (1982). Submitted to *Acta Cryst. B*.

HEWAT, A. W. & BAILEY, I. (1976). *Nucl. Instrum. Methods*, **137**, 463–471.

HOWE, A. T. & SHILTON, M. G. (1979). *J. Solid State Chem.* **28**, 345–361.

HOWE, A. T. & SHILTON, M. G. (1980). *J. Solid State Chem.* **34**, 149–155.

KÄNZIG, W. (1957). In *Solid State Physics*, edited by F. SEITZ and D. TURNBULL, Vol. 4, p. 124. New York: Academic Press.

KUHS, W. F. & LEHMANN, M. S. (1981). *Nature (London)*, **294**, 432–434.

LUNDGREN, J. O. & OLOVSSON, I. (1967). *Acta Cryst.* **23**, 966–971.

MOROSIN, B. (1978*a*). *Acta Cryst.* B**34**, 3732–3734.

MOROSIN, B. (1978*b*). *Phys. Lett. A*, **65**, 53–54.

PETERSON, S. W. & LEVY, H. A. (1957). *Acta Cryst.* **10**, 70–76.

RIETVELD, H. M. (1967). *Acta Cryst.* **22**, 151–152.

RIETVELD, H. M. (1969). *J. Appl. Cryst.* **2**, 65–71.

SAKATA, M. & COOPER, M. J. (1979). *J. Appl. Cryst.* **12**, 554–563.

SHILTON, M. G. & HOWE, A. T. (1977). *Mater. Res. Bull.* **12**, 701–706.

SHILTON, M. G. & HOWE, A. T. (1979). *Chem. Commun.* pp. 194–196.

SHILTON, M. G. & HOWE, A. T. (1980). *J. Solid State Chem.* **34**, 137–147.

THOMAS, J. O. & LIMINGA, R. (1978). *Acta Cryst.* B**34**, 3686–3690.

THOMAS, M. W. & BENDALL, P. J. (1978). *Acta Cryst.* A**34**, S351.

ZHELUDEV, I. S. (1971). *Solid State Physics*, edited by H. EHRENREICH, F. SEITZ & D. TURNBULL, Vol. 26, p. 454. New York: Academic Press.